SIMULATION OF SOLAR-INDUCED CHLOROPHYLL FLUORESCENCE FROM 3D CANOPIES WITH THE DART MODEL

O. Regaieg[1], Wang Y.[1], Z. Malenovsky[2,3], T. Yin[3,5], A. Kallel[4], J. Duran N.[1,5], Delavois A.[1], J. Qi[1,6], E. Chavanon[1], N. Lauret.[1], J. Guilleux[1], B. Cook[7], D. Morton[7], Gastellu-Etchegorry J.P.[1]

1. CESBIO - UPS, CNES, CNRS, IRD, Université de Toulouse, 31401 Toulouse cedex 9, France.
2. School of Technology Engineering and Design, University of Tasmania, Hobart, Australia
3. Earth System Science Interdisciplinary Center, University of Maryland, College Park, MD 20740-3823, USA
4. CRNS, ATMS, Sfax, Tunisia – 5. Magellium, 31520 - Ramonville Saint-Agne, France
6. College of Remote Science and Engineering, Beijing Normal University, China
7. NASA Goddard Space Flight Center, Greenbelt, MD 20771, USA

IGARSS 2020 - 2020 IEEE International Geoscience and Remote Sensing Symposium | 978-1-7281-6374-1/20/$31.00 ©2020 IEEE | DOI: 10.1109/IGARSS39084.2020.9323616

ABSTRACT

The potential of solar-induced chlorophyll fluorescence (SIF) to monitor photosynthesis and plant stress has attracted considerable interest in SIF remote sensing (RS). However, canopy SIF and RS observations are impacted by topography, vegetation three dimension (3D) structure, leaf orientation, non foliar elements (e.g., tree woody skeleton),… Physically based downscaling of canopy SIF RS data to leaf-level (i.e., to leaf photosynthesis) requires 3D radiative transfer (RT) models simulating canopy SIF and its observation. These models are necessary to better exploit the potential of SIF, by linking leaf SIF and SIF in RS observations as a function of canopy 3D architecture and experimental configurations (sun and viewing directions, etc.). The Discrete Anisotropic Radiative Transfer (DART) model is a comprehensive 3D radiative transfer (RT) model for urban and natural landscapes. This paper presents its SIF modeling for vegetation simulated with facets, its validation with the SCOPE/mSCOPE 1D models, and its recent extension to SIF modelling for landscapes simulated with 3D turbid medium.

Index Terms— Radiative transfer, DART, SIF, 3-D vegetation, turbid, facet, optical remote sensing.

1. INTRODUCTION

SIF is a spontaneous radiation re-emission by plants in the red - near-infrared domain [640-850nm] induced by absorption of 400-750nm radiation. SIF yield is a small fraction of the absorbed PAR (APAR). It is in competition with both the photosynthetic process (*i.e.*, photochemical quenching) and heat dissipation (*i.e.*, non-photochemical quenching). SIF is viewed as a reliable and real-time process-based indicator of the functional state of photosynthesis [1]. Indeed, unlike standard reflectance vegetation indices (*e.g.*, NDVI: Normalized Difference Vegetation Index), it reacts rapidly to changing environmental conditions and stress factors [2].

The potential of SIF for detecting vegetation stress and to study the carbon cycle has triggered huge interest in the scientific community to further study this phenomenon using RS observations. Several techniques were developed to retrieve SIF from the atmospheric O_2-B (687 nm) and O_2-A (760 nm) absorption bands [3]. In this context, the satellite mission FLEX (Fluorescence Explorer), dedicated to the observation of SIF from space, is planned to be launched in 2024 by the European Space Agency (ESA).

Models that simulate canopy SIF and its RS observation are needed to better understand and exploit the potential of SIF. SCOPE [4] is the reference model for SIF simulation of one dimensional (1D), homogeneous canopies. It was recently extended to simulate SIF from vertically heterogeneous canopies (*i.e.*, mSCOPE [5]). However, it remains a 1D model. The 3D structure of vegetation strongly influences the SIF signal. Therefore, 3D physical models, such as DART [5], are needed to downscale canopy SIF to leaf SIF as a function of canopy 3D structure, illumination conditions, and sensor characteristics. Here, we present recent advances concerning SIF modeling in DART.

DART is a comprehensive, physically-based 3D RT model developed by CESBIO since 1993 (dart.omp.eu). It models RT in vegetation and urban landscapes, and also in the atmosphere, with the so-called flux tracking method. It simulates accurately TOA and BOA RS observations and the radiative budget (RB) in the visible, near-infrared and thermal-infrared spectral domains for any experimental and instrument configuration (sun direction, viewing direction, atmosphere, spatial resolution, …) as acquired by imaging spectro-radiometers and LiDAR (Light Detection And Ranging), sensors (scanners, cameras, …) from satellite, airborne, or in situ sensors. SIF modelling was first introduced in DART for vegetation canopies simulated with facets [6]. Below, we present its validation with the SCOPE model, and its extension to vegetation simulated with turbid medium.

2. SIF MODELINGOF FACET BASED VEGETATION

DART simulates leaf SIF (*i.e.*, leaf backward / forward SIF of photosystems I & II, hereafter PSI and PSII) with the embedded FLUSPECT model [7], and optionally with SCOPE

Eta matrices that weight leaf SIF to consider environmental factors (*e.g.*, temperature). It simulates the total and 3D SIF emitted in the canopy, as well as BOA and TOA canopy SIF observations.

Unlike the probabilistic treatment of sunlit and shaded leaves in SCOPE (*i.e.*, the proportion of sunlit and shaded leaves is defined by the instantaneous sun direction), DART can simulate past and present leaf irradiance to identify sun- and shade-adapted leaves. DART first computes the irradiance of all leaves over a user selected period, and then classifies leaves as sun- and shade-adapted leaves, i.e. leaves with the pigment pool and photoprotective mechanisms adapted to the prevailing incoming irradiation intensity. It results in a 3D canopy object with at least two groups (i.e., sun- and shade-adapted leaves) to which specific biochemical properties and fluorescence yields are assigned.

SCOPE was used to assess validity of DART SIF simulations. Because SCOPE works only with vegetation simulated as horizontally homogeneous turbid medium, DART was run with a so-called quasi-turbid medium: volume filled with a very large number of very small facets having the same Leaf Area Index and Leaf Angle Distribution as the turbid medium representation in SCOPE.

SCOPE canopy SIF modelling relies on the simulation of the canopy energy budget (EB), which gives the vertical profile of temperature. The EB depends on many factors and mechanisms: incident sun and atmosphere radiation, leaf photosynthesis and evapotranspiration, meteorological parameters, soil reflectance, etc. SCOPE uses this bioclimatic information to weight the leaf SIF simulated by the FLUSPECT model with the so-called Eta factors. These factors are specific for sunlit and shaded leaves. DART cannot calculate canopy bioclimatic conditions since it is not an EB model. Therefore, a model coupling strategy was adopted: SCOPE was modified to export the Eta factors, and DART was modified to import and to manage them.

$DART_{facet}$ - SCOPE comparisons were conducted with equal proportions of sunlit and shaded leaves in each model. Many configurations were tested. Figure 1 shows a comparison of $DART_{facet}$ and SCOPE canopy SIF. Input parameters are listed in Table 1. Three cases are considered:

- EB_{SCOPE} is off: DART and SCOPE use Eta=1 (Fig. 1.a).
- EB_{SCOPE} is on, and DART uses Eta=1 (Fig. 1.b). This case illustrates the impact of SCOPE EB (i.e., Eta factors) on canopy SIF emission and radiance. The resulting mean absolute relative error (MARE) is larger than 12%.
- EB_{SCOPE} is on, and DART uses SCOPE Eta factors (Fig. 1.c)

The SCOPE EB only impacts PSII, since in SCOPE PSI does not depend on environmental conditions. Whenever DART uses the SCOPE Eta factors, the MARE is smaller than 3% for total canopy SIF, and smaller than 6% for SIF radiance.

Figure 1.d plots the total SIF emitted within the canopy. It is used to compute the canopy escape factor $\frac{Canopy\ SIF\ exitance}{Total\ canopy\ SIF}$. It appears that if DART and SCOPE use the same Eta factors, the DART and SCOPE canopy total SIF are nearly equal. It indicates that the small residual differences between the DART and SCOPE canopy SIF exitance / radiance values are probably explained by:

- DART and SCOPE different RT algorithm: flux tracking in DART and differential equations in SCOPE.
- Multiple scattered radiation is assumed to be isotropic in SCOPE, whereas it is anisotropic in DART.

Table 1. DART and SCOPE simulations input parameters.

Chlorophyll content (Cab)	60 µg/cm^2
Carotenoid content (Cca)	15 µg/cm^2
Water content (Cw)	0.008 cm
Dry matter content (Cdm)	0.002 g/cm^2
Senescent material fraction (Cs)	0
Anthocyanin content (Cant)	0 µg/cm^2
Structure coefficient (N)	1.5
Leaf area index (LAI)	3
PSI quantum yield (PSI Fqe)	0.006
PSII quantum yield (PSII Fqe)	0.03
Sun direction (θ_s, ϕ_s)	(30°, 225°)
Viewing direction (θ_v, ϕ_v)	(0°, 0°)
Ground reflectance (ρ_g)	0

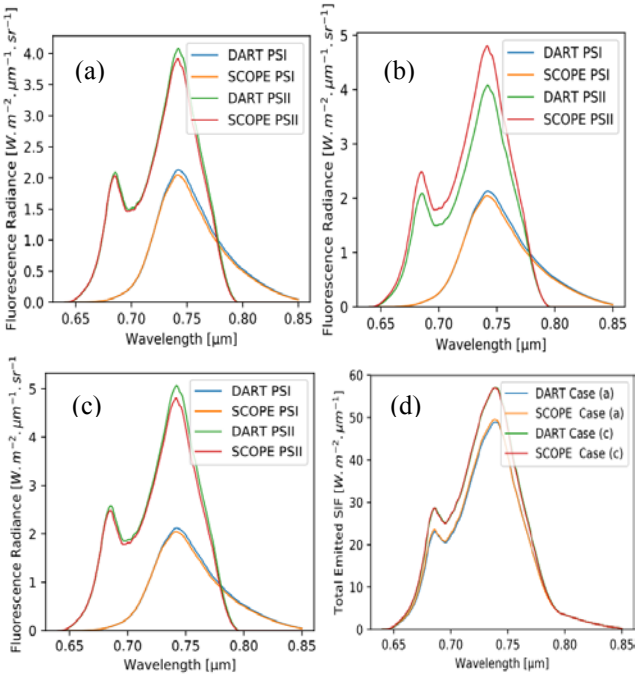

Fig. 1. $DART_{facet}$ and SCOPE SIF. a) Canopy radiance: SCOPE energy balance is off. b) Canopy radiance: SCOPE energy balance is on, and DART uses Eta=1. c) Canopy radiance: SCOPE energy balance is on and DART uses the SCOPE Eta factors. d) Total within canopy emitted SIF with same Eta factors for DART and SCOPE.

mSCOPE [7], an extension of the SCOPE model, which operates with vertical heterogeneity of the biophysical and

biochemical properties of vegetation. DART$_{facet}$ agrees with mSCOPE for this multi-layered canopy, similarly as in the 1D SCOPE comparison (MARE<3%). Figure 3 illustrates this result for the case of a three-layer canopy (Table 2), for cases with and without the SCOPE EB.

Table. 2. DART and mSCOPE simulations input parameters.

	Top	Middle	Bottom
Cab	40 µg/cm^2	60 µg/cm^2	80 µg/cm^2
Cca	10 µg/cm^2	15 µg/cm^2	20 µg/cm^2
Cw	0.006 cm	0.01 cm	0.012 cm
Cdm	0.0014 g/cm^2	0.002 g/cm^2	0.0028 g/cm^2
Cs	0	0	0
Cant	0 g/cm^2	0 g/cm^2	0 g/cm^2
N	1	1.5	2
LAI	0,6667	0,6667	0.6667
PSI Fqe	0.006		
PSII Fqe	0.03		
(θ_s, ϕ_s)	(37.94°,311.89°)		
(θ_v, ϕ_v)	(0°,0°)		
ρ_g	0		

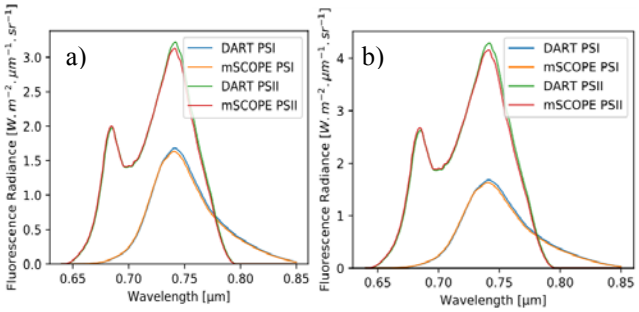

Fig. 2. DART$_{facet}$ and mSCOPE SIF results comparison with the SCOPE energy balance off (a), and on (b) with SCOPE Eta factors used by DART.

In summary, DART$_{facet}$ and SCOPE/mSCOPE are very close. However, as expected, differences are larger for cases with realistic canopies, as illustrated by Figure 3, with even larger differences for complex 3D forest canopies.

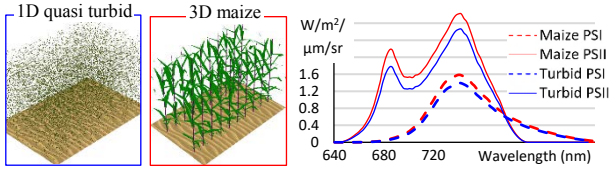

Fig. 3. DART$_{facet}$ SIF: 3D maize vs. equivalent 1D turbid canopy

3. SIF MODELING IN 3D TURBID VEGETATION

The simulation of landscapes with facets is very accurate but can be very computationally intensive. The use of turbid cells (*i.e.*, cells filled with turbid medium) can reduce this constraint. This way, it provides a solution for simulating SIF across large and spatially heterogeneous landscapes, while preserving their 3D architecture. With this objective in mind, DART SIF modelling was recently extended to the case of vegetation simulated with turbid cells. Figure 4 illustrates radiation mechanisms in a turbid cell, including PSx SIF emission, where PSx stands for PSI and PSII. It represents a very simple case: the incident radiation [$W_{in}(\lambda_j,\Delta\Omega_s)$] and all emitted SIF are at the same wavelength λ_j. Scattering at $M^{\uparrow}$ gives rise to the single scattered flux $\{\boldsymbol{w}_1(\lambda_j,\Omega_v), \boldsymbol{w}_{1,PS1}(\lambda_j,\Omega_v), \boldsymbol{w}_{1,PS2}(\lambda_j,\Omega_v)\}$. $\boldsymbol{w}_{1,\alpha}(\lambda_j,\Omega_v)$ is the part of $\boldsymbol{w}_1(\lambda_j,\Omega_v)$ that escapes the cell without further scattering. Therefore, $\frac{\boldsymbol{w}_{1,\alpha}(\lambda_j,\Delta\Omega_v)}{\boldsymbol{w}_1(\lambda_j,\Delta\Omega_v)}.\boldsymbol{w}_{1,PSx}(\lambda_j,\Omega_s)$ is the part of $\boldsymbol{w}_{1,PSx}(\lambda_j,\Omega_v)$ that escapes the cell without further scattering. Similarly, the radiation scattered at $M^{\uparrow}$ gives rise to multiple scattering, and the resulting radiation that exits the cell is noted $\boldsymbol{w}_{1,\beta}(\lambda_j,\Omega_v)$. The associated SIF radiation that exits the cell is $\frac{\boldsymbol{w}_{1,\beta}(\lambda_j,\Delta\Omega_v)}{\boldsymbol{w}_1(\lambda_j,\Delta\Omega_v)}.\boldsymbol{w}_{1,PSx}(\lambda_j,\Omega_s)$. The following tree within-cell SIF emission mechanisms are considered:

1) $\boldsymbol{w}_{1,PSx}(\lambda_j,\Omega_v)$: SIF emission along the direction of incident radiation intercepted along the path AB: Direct interception of radiation incident on the cell
2) $\boldsymbol{w}_{1,int,PSx,\gamma}(\lambda_j,\Omega_s)$: SIF (re-)emission due to absorption of multiple scattering of incident radiation [$W_{in}(\lambda_j,\Delta\Omega_s)$].
3) 3rd order and higher order SIF emission due to the absorption of SIF that is re-emitted within the cell. These SIF orders larger than 2 are small enough to be neglected.

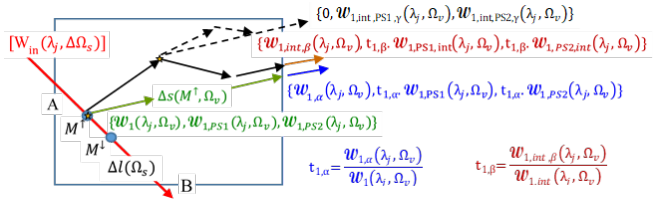

Fig 4. DART incident radiation [$W_{in}(\lambda_j,\Delta\Omega_s)$] into a turbid cell, with source points $M^{\uparrow}$ and $M^{\downarrow}$, and energy $\{\boldsymbol{w}_1(\lambda_j,\Omega_v), \boldsymbol{w}_{1,PS1}(\lambda_j,\Omega_v), \boldsymbol{w}_{1,PS2}(\lambda_j,\Omega_v)\}$ from $M^{\uparrow}$. $\Delta l(\Omega_s)$ is the distance between the entry A and exit B of the incident ray. $\Delta s(M^{\uparrow},\Omega_v)$ is the distance between $M^{\uparrow}$ and the cell exit along direction Ω_v. $\boldsymbol{w}_{1,\alpha}(\lambda_j,\Omega_v)$ is equal to the direct transmission of $\boldsymbol{w}_1(\lambda_j,\Omega_v)$ outside the cell without any scattering, whereas $\boldsymbol{w}_{1,int,\beta}(\lambda_j,\Omega_v)$ is the transmission of $\boldsymbol{w}_1(\lambda_j,\Omega_v)$ outside the voxel with scattering events.

The 1st order SIF emitted energy $\boldsymbol{w}_{1,PSx}(\lambda_j,\Omega_v)$, due to intercepted energy $\boldsymbol{w}_{int}(\lambda_i,\Omega_s)$ from [$W_{in}(\lambda_j,\Delta\Omega_s)$] is:

$$\boldsymbol{w}_{1,PSx}(\lambda_j,\Omega_v) = \sum_i \boldsymbol{w}_{int}(\lambda_i,\Omega_s).T_{PSx}(\lambda_i,\lambda_j,\Omega_s,\Omega_v)$$

with $T_{PSx}(\lambda_i,\lambda_j,\Omega_s,\Omega_v)$ the turbid medium SIF transfer function, for incident band λ_i, and emission band λ_j.

The intercepted energy due to the direct transmission of $\boldsymbol{w}_1(\lambda_j,\Omega_v)$ is:

$$\boldsymbol{w}_{1,\mathrm{int}}(\lambda_j,\Omega_s) = \sum_{v=1}^{N_{dir}} [\boldsymbol{w}_1(\lambda_j,\Omega_v) - \boldsymbol{w}_{1,\alpha}(\lambda_j,\Omega_v)]$$

with the assumption that within cell scattered radiation intensity is isotropic, the total energy that escapes the cell after within-cell single and multiple scattering is:

$$\boldsymbol{w}_{1,\mathrm{int},\beta}(\lambda_j,\Omega_s) = \boldsymbol{w}_{1,\mathrm{int}}(\lambda_j,\Omega_s).\frac{\omega_j.<T>}{1-\omega_j.[1-<T>]}$$

with $<T>$ the mean within cell transmittance along paths $\Delta m(\Omega)$ from the cell center to the cell faces, and ω_j the single scattering albedo for λ_j.

Hence, the within cell absorbed energy due to the propagation of rays $\boldsymbol{w}_1(\lambda_j,\Omega_s \rightarrow \Omega_v)$ is:

$$\boldsymbol{w}_{1,\mathrm{abs}}(\lambda_j,\Omega_s) = \boldsymbol{w}_{1,\mathrm{int}}(\lambda_j,\Omega_s) - \boldsymbol{w}_{1,\mathrm{int},\beta}(\lambda_j,\Omega_s)$$

This absorbed energy gives rise to PSI and PSII SIF emitted energy. With the assumption that rays that have been scattered at least 2 times in the cell are isotropic, we obtain:

$$\boldsymbol{w}_{1,\mathrm{int,PSx}}(\lambda_k,\Omega_s) = \sum_j 2.\frac{\boldsymbol{w}_{1,abs}(\lambda_j,\Omega_s)}{1-\omega_j}.\mathrm{M_{PSx}}(\lambda_j,\lambda_k)$$

The factor 2 is given by the fact the absorption of an incident ray that gives rise to forward and backward SIF. $\mathrm{M_{PSx}}(\lambda_j,\lambda_k)$ is the mean value of the spectrally-scaled FLUSPECT matrices in DART. So, the resulting 2nd order PSx energy that exits the cell is:

$$\boldsymbol{w}_{1,\mathrm{int,PSx},\gamma}(\lambda_k,\Omega_s) = \boldsymbol{w}_{1,\mathrm{int,PSx}}(\lambda_k,\Omega_s).\frac{<T>}{1-\omega_k.(1-<T>)}$$

$\mathrm{DART_{turbid}}$ SIF was tested and compared with $\mathrm{DART_{facet}}$ for several configurations. MARE was in all cases around 1%. The comparison, using input parameters in Table 1, is depicted in Figure 5.

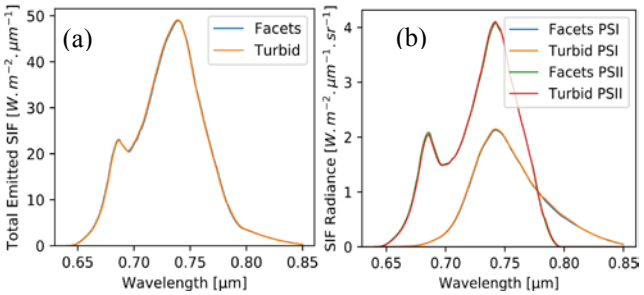

Fig. 5. $\mathrm{DART_{facet}}$ and $\mathrm{DART_{turbid}}$ canopy total emitted SIF(left) and canopy SIF radiance (right).

4. CONCLUDING REMARKS

DART simulates SIF emitted from a canopy, and also BOA and TOA SIF hyperspectral measurements and images for any canopy configuration simulated either with facets or 3D turbid medium. Its coupling with SCOPE allowed us to consider the impact of environmental parameters on the SIF emissions of sunlit and shaded leaves.

Further validation of DART SIF modeling with in-situ and RS measurements is required to confirm its reliability and broad applicability.

Three on-going improvements in DART will also improve SIF modelling:

- Novel Monte Carlo methods to simulate fast images (DART Lux). The DART Lux mode will efficiently simulate hyperspectral SIF images of large facet- and turbid-created landscapes (extent of several km). Since Monte Carlo methods are not adapted to the simulation of the total within canopy SIF, a dual modelling approach is planned: DART flux tracking for simulating total canopy SIF and DART Lux for simulating canopy SIF images.
- Implementation of 3D energy balance model that would directly compute the factors that affect SIF production.
- Coupling of DART with a 3D SIF leaf model [10].

5. ACKNOWLEDGMENTS

This work was supported by the Centre National d'Etudes Spatiales (CNES), with TOSCA project 'Fluo3D' and by NASA through internal funding 'Scaling Solar Induced Fluorescence from Leaves to Landscapes'. Contribution of Z. Malenovský was supported by the Australian Research Council Future Fellowship project (FT160100477) 'Bridging scales in remote sensing of vegetation stress'.

6. REFERENCES

[1] Baker N.R. Chlorophyll fluorescence: a probe of photosynthesis in vivo. Annu. Rev. Plant Biol. 59, 89-113. 2008.

[2] Alonso L., Van Wittenberghe S. et al. Diurnal cycle relationships between passive fluorescence, PRI and NPQ of vegetation in a controlled stress experiment. Remote Sensing. 9(8): 770. 2017.

[3] Daumard, F., Champagne, S., Fournier, A., Goulas, Y., Ounis, A., Hanocq, J.F., Moya, I. A field platform for long-term measurement of canopy fluorescence. IEEE Transaction on Geosciences and Remote Sensing 48 (9), 3358–3368. 2010.

[4] van der Tol, C., Verhoef, W., Timmermans, J., Verhoef, A., and Su,Z. An integrated model of soil-canopy spectral radiances, photosynthesis, fluorescence,temperature and energy balance. Biogeosciences, 6:3109–3129. 2009.

[5] Yang, P., Verhoef, W., and van de Tol, C. The mSCOPE model: A simple adaptation of the scope model to describe reflectance, fluorescence and photosynthesis of vertically heterogeneous canopies. Remote Sensing of Environment, 201:1–11. 2017.

[6] Gastellu-Etchegorry, J. P., Yin, T., Lauret, N. et al. Discrete anisotropic radiative transfer (DART 5) for modelling airborne and satellite spectroradiometer and LiDAR acquisitions of natural and urban landscapes. Remote Sensing, 7(2), 1667–1701. 2015.

[7] Gastellu-Etchegorry J.P. et al. DART: recent advances in remote sensing data modeling with atmosphere, polarization, and chlorophyll fluorescence. IEEE JSTARS, 10(6), 2640-49. 2017.

[8] Vilfan, N., van der Tol, C., Muller, O., Rascher, U., and Verhoef, W. Fluspect-B: A model for leaf fluorescence, reflectance and transmittance spectra. Remote Sensing Env., 186:596-615. 2016.

[9] Malenovský Z. et al. Cross validation of DART and SCOPE models. Remote Sensing. Preparation.

[10] Kallel A. Leaf polarized BRDF simulation based on Monte Carlo 3-D vector RT modeling. Journal of Quantitative Spectroscopy and Radiative Transfer. 221: 202-224. 2018.